33rd Annual International Conference of the IEEE EMBS
Boston, Massachusetts USA, August 30 - September 3, 2011

Accuracy and repeatability of parameter estimation methods from ambulatory data for the wrist joint

Mohammad Esmaeili, Sarah Moussouni, Ferdinan Widjaja, Kumudu Gamage, Domenico Campolo
School of Mechanical and Aerospace Engineering, Nanyang Technological University, 639798 Singapore

***Abstract*—In this paper, as a preliminary study, we show that accuracy and repeatability in ambulatory measurements of wrist joint are related to movement conditions which are going to be used in a calibration procedure. We chose two representative in-vivo, non-invasive calibration methods of the human upper limb, from those available in literature, to estimate joint parameters. Developing an analytical model of wrist joint we used sets of synthetic data each of which containing different number of samples, joint covariations and noise to estimate the repeatability and accuracy of the methods in estimation. Afterwards, we used our mechanical mock-up to examine single joint motions as well as the rotation of both joints (i.e. flexion-extension rotation and radial-ulnar deviation) on accuracy and repeatability by calculating the mean and standard deviation of the relative errors. Finally, we show that the accuracy of adapted method (its relative error was less than 7%) is better than the other method in estimating the joint parameters.**

I. Introduction

Kinematic analysis of the upper limb is nowadays a fundamental tool in various medical fields, in particular clinical applications. Also thanks to the recent boost of technology available for motion tracking [1] low-cost, ambulatory, non-invasive assessment of arm kinematics is now at reach [2].

Many studies have focused on the shoulder-elbow complex while relatively fewer addressed the wrist joint, despite its importance on activities of daily living [3], [4], [5], [6], [7], [8]. Based on both in-vivo and in-vitro studies, it is considered an acceptable simplification to model the human wrist as a universal joint with two axes: the flexion-extension axis (FE), proximal and fixed in the forearm, and the radial-ulnar deviation (RUD) axis, distal and fixed in the hand. These two axes are skew-oblique, typically offset by few millimeters and approximately orthogonal [9].

Ambulatory assessment would in general make use of wearable sensors to be strapped onto the subject. In the case of the wrist, sensors shall be placed on the forearm and on the hand (see Fig. 1.a). To minimize skin motion, bony areas such as the distal, dorsal part of the forearm are preferred for strapping. Once the sensors are in place, a calibration procedure involving voluntary or induced motions of one or more joints is necessary to determine the relative positions and orientations between anatomical features (FE and RUD axes) and the sensors. Only after a calibration procedure one will be able to infer the anatomical joint angles from sensors readings. Calibration is therefore a crucial step as its accuracy will directly affect the accuracy of the final kinematic analysis.

In the specific case of in-vivo, non-invasive calibration methods suitable to ambulatory settings, several calibration methods have been proposed for the joints of the human upper limb[1][10], [11], [12], [2], [13]. Many similarities exist among these approaches in the sense a serial kinematic chain with unknown parameters is assumed to model the human upper limb (or a subset of its joints) and optimal estimates for the unknown parameters are derived from measurements in a least-squares framework.

In this work, we are primarily interested in how joint covariation as well as noise in measurements may influence the outcome of calibration methods. Unlike the elbow, the two joints of the wrist are actuated by the same set of muscles and voluntary movements can hardly produce pure single-joint motions [14]. Some calibration methods rely on single-joint movements and therefore might provide erroneous estimates due to such a covariation. Conversely, other methods devised to assess multiple joints at a time, might provide erroneous results when one of the joints is not sufficiently involved.

To this end, we selected two representative methods from those available in literature focusing on the two skew-oblique axes of the wrist: the first method (M1) was proposed by Biryukova et al. [10] and was devised to estimate parameters for one joint at a time; the second method (M2) is adapted from Prokopenko et al. [12] is used to estimate all parameters at once. The reason for readapting the second method is that in the original work [12], the authors minimize the so called 'Direct Kinematic Error', which is a weighted sum of position errors and orientation errors (between estimated and measured data). This step necessarily involves a somewhat arbitrary choice of weights, Prokopenko et al. [12] justify this choice based on a specific set of data but it is clearly movement dependent. In this paper we shall use for both methods M1 and M2 the same least-square approach used in [10]. Therefore, the method M1 is implemented 'as is', see [10] for details, while for method M2 we provide a detailed description of our implementation, to enable the reader to reproduce the algorithm.

Non-invasive calibration methods proposed in literature, are typically tested on several subjects over multiple trials. Due to various sources of errors (e.g noisy measurements and skin

Corresponding author is D. Campolo, email: d.campolo@ntu.edu.sg.
This work is supported by the Academic Research Fund (AcRF) Tier1 (RG 40/09), Ministry of Education, Singapore.

[1]The shoulder is regarded as ball-in-socket joint, while the remaining joints at elbow and wrist are regarded as rotational hinges.

978-1-4244-4122-8/11/$26.00 ©2011 IEEE

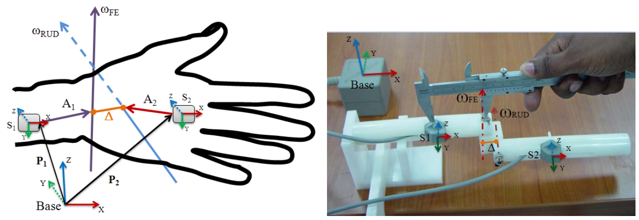

a) b)

Fig. 1. Axes of rotation in the wrist joint in human wrist (a) and mechanical mock-up counterparts (b). $\boldsymbol{P}_1$ and $\boldsymbol{P}_2$ are the position vectors of the sensor S_1 on the forearm and S_2 on the 3^{rd} metacarpal in the stationary frame, *Base*; $\boldsymbol{A}_1$ and $\boldsymbol{\omega}_{FE}$ are the position vector and orientation of the FE axis relative to the S_1; $\boldsymbol{A}_2$ and $\boldsymbol{\omega}_{RUD}$ are the position vector and orientation of the RUD axis relative to the S_2 pointing to the minimal distance Δ between the two axes.

motion) different estimates are obtained from different trials. The standard deviation of the parameters across trials or the small residuals in the fitting process [12] are often taken as an index of accuracy. In fact, standard deviation or goodness of fit are index of repeatability but not accuracy, as the ground-truth is not known (only invasive methods can be used to measure the real anatomical features). In this work, we shall test the two representative methods M1 and M2 on a set of synthetic data as well as on real data acquired via a mechanical mock-up (shown in Fig. 1.b). In both cases the ground-truth, i.e. the actual geometry of the problem, is known and therefore accuracy can be determined. The synthetic approach allows to generate ideal as well as noisy data, the mechanical mock-up involves the real sensors with their specific noise levels and allows to test the calibration methods without incurring in other nonidealities such as skin motion.

The paper is organized as follows. In section II, the kinematic model for wrist joint is described. Section III presents the adapted method for M2 as well as approaches which we considered for synthetic and experimental data to evaluate the proposed methods. Finally, the effects of different motion conditions are presented and discussed.

II. Wrist Kinematic Model

The wrist model considered here is as in [10], [12]: a universal joint with two skew-oblique axes, as in Fig. 1.a. The unit vector $\boldsymbol{\omega}_{FE}$ represents the FE axis and is fixed on the forearm, i.e. proximally. The unit vector $\boldsymbol{\omega}_{RUD}$ represents the RUD axis and is fixed on the hand, i.e. distally. The two axes are non intersecting, with a few millimeters distance Δ between them [3], and approximately perpendicular, although variations exist from subject to subject. The Range of Motion (RoM) of the joint angles θ_{FE} and θ_{RUD} also may vary from subject to subject but, on average, can be considered as [-50 35] degrees for θ_{RUD} and [-65 70] degrees for θ_{FE}.

Fig. 1.a, also shows the main frames of interest in this problem. Two sensors, attached to the forearm and to the hand, define two frames of reference S1 and S2, respectively, as in Fig. 1.a. We used the Liberty System (Polhemus Technologies Inc), for which each electromagnetic sensor provides readings of its orientation and position (6 degrees of freedom) with respect to a base frame of reference B (corresponding to the electromagnetic source) and a rate of 240 samples per second. Both sensors and source are visible in Fig. 1.b where the source is the large cube and the sensors are fixed onto the mock-up.

It should be noticed that $\boldsymbol{\omega}_{FE}$ is fixed with respect to S1, while $\boldsymbol{\omega}_{RUD}$ is fixed with respect to S2. According to the anatomical structure of the wrist, we defined an additional frame (f_{FE}). Its x-axis is aligned with $\boldsymbol{\omega}_{FE}$, its z-axis is aligned with $\boldsymbol{\omega}_{FE} \times \boldsymbol{\omega}_{RUD}$, i.e. perpendicular with both FE and RUD axes, and its y-axis is defined via the right-hand rule.

Following standard robotics approaches [15], we can now define the transformations between the above defined reference frames, with the convention that a symbol ${}^{A}T_{B}$ indicates a 4×4 homogeneous transformation matrix from a frame B into a frame A, a bold symbol $\boldsymbol{X}$ indicates a space vector and $\boldsymbol{X}^{(F)}$ indicates its coordinates with respect to a frame F.

In ambulatory conditions, sensors S1 and S2 will provide time-varying readings ${}^{B}T_{S1}$ and ${}^{B}T_{S2}$, respectively:

$$ {}^{B}T_{Si} = \begin{bmatrix} R_i & \boldsymbol{P}_i^{(B)} \\ 0\ 0\ 0 & 1 \end{bmatrix} \tag{1} $$

Where $i = 1, 2$, R_i is the rotation matrix and $\boldsymbol{P}_i^{(B)}$ the position of sensor S_i with respect to the base (B).

Nevertheless, such readings will not be independent because of the kinematic relationship between the two sensors:

$$ {}^{B}T_{S2} = {}^{B}T_{S1}\ {}^{S1}T_{f_{FE}}\ {}^{f_{FE}}T_{S2} \tag{2} $$

Following [15] ${}^{S1}T_{f_{FE}}$, ${}^{f_{FE}}T_{S2}$ in (2) are defined as :

$$ {}^{f_{FE}}T_{S2}(\theta_{RUD}) = \exp(\widehat{\xi}_{RUD}\theta_{RUD})\, {}^{f_{FE}}T_{S2}(0) \tag{3} $$
$$ {}^{S1}T_{f_{FE}}(\theta_{FE}) = \exp(\widehat{\xi}_{FE}\theta_{FE})\, {}^{S1}T_{f_{FE}}(0) \tag{4} $$

Where the exponential $\exp \widehat{\xi}\theta$ in (3)-(4) defines a *screw motion* generated by a *twist* $\widehat{\xi}$, operatively defined as

$$ \widehat{\xi} = \begin{bmatrix} \widehat{\omega} & \boldsymbol{v} \\ 0 & 0 \end{bmatrix} = \begin{bmatrix} \widehat{\omega} & -\boldsymbol{\omega} \times \boldsymbol{q} + h\boldsymbol{\omega} \\ 0 & 0 \end{bmatrix} \tag{5} $$

Where $\boldsymbol{\omega}$ is the unit vector of a rotation axis; q is any point on the axis; h is the pitch[2]; and $\boldsymbol{v} = -\boldsymbol{\omega} \times q + h\boldsymbol{\omega}$.

For rotational axes ($\boldsymbol{\omega} \neq \boldsymbol{0}$) the exponential is computed as

$$ e^{\widehat{\xi}\theta} = \begin{bmatrix} e^{\widehat{\omega}\theta} & (I - e^{\widehat{\omega}\theta})(\boldsymbol{\omega} \times \boldsymbol{v}) + \boldsymbol{\omega}\boldsymbol{\omega}^T \boldsymbol{v}\theta \\ 0 & 1 \end{bmatrix} \tag{6} $$

Table I provides the parameters used for the numerical calculations considering the position vectors $\boldsymbol{A}_1$ in (S1) and $\boldsymbol{A}_2$ in (S2) defined as

$$ \boldsymbol{A}_1^{(S1)} := [A_{1x}\ A_{1y}\ A_{1z}]^T;\ \boldsymbol{A}_2^{(S2)} := [A_{2x}\ A_{2y}\ A_{2z}]^T \tag{7} $$

[2]For purely rotational joints h = 0. In our current mechanical mock-up, the rotational joints are implemented with low-pitch screws and we neglected any pitch effect.

and the distance between the FE and RUD axes geometrically defined as

$$\boldsymbol{\Delta} = \Delta \frac{\boldsymbol{\omega}_{FE} \times \boldsymbol{\omega}_{RUD}}{|\boldsymbol{\omega}_{FE} \times \boldsymbol{\omega}_{RUD}|} \tag{8}$$

with $\boldsymbol{\Delta}^{(f_{FE})} = [\Delta_x \ \Delta_y \ \Delta_z]^T$.

TABLE I
PARAMETERS FOR THE SCREW MOTION CALCULATION

	$\boldsymbol{\omega}$	q	${}^{A}T_B(0)$
${}^{S1}T_{f_{FE}}$	$\begin{bmatrix} 0 \\ -1 \\ 0 \end{bmatrix}$	$\begin{bmatrix} A_{1x} \\ A_{1y} \\ A_{1z} \end{bmatrix}$	$\left[\begin{array}{ccc\|c} 0 & 0 & 1 & A_{1x} \\ -1 & 0 & 0 & A_{1y} \\ 0 & -1 & 0 & A_{1z} \\ \hline & 0 & & 1 \end{array}\right]$
${}^{f_{FE}}T_{S2}$	$\begin{bmatrix} 0 \\ 1 \\ 0 \end{bmatrix}$	$\begin{bmatrix} \Delta_x + A_{2y} \\ \Delta_y + A_{2z} \\ \Delta_z - A_{2x} \end{bmatrix}$	$\left[\begin{array}{ccc\|c} 0 & -1 & 0 & \Delta_x \\ 0 & 0 & -1 & \Delta_y \\ 1 & 0 & 0 & \Delta_z \\ \hline & 0 & & 1 \end{array}\right]$

III. METHODS

A. Parameter Estimation

Referring to Fig. 1.a, the following invariant i.e. frame independent) geometric relation holds:

$$\boldsymbol{P}_2 - \boldsymbol{P}_1 = \boldsymbol{A}_1 + \boldsymbol{\Delta} - \boldsymbol{A}_2 \tag{9}$$

Vectors $\boldsymbol{P}_1$ and $\boldsymbol{P}_2$ are conveniently expressed in base frame (B) coordinates, as the sensors directly measure $\boldsymbol{P}_1^{(B)}$ and $\boldsymbol{P}_2^{(B)}$. Vector $\boldsymbol{A}_1$ and $\boldsymbol{\omega}_{FE}$ are unknown but, being fixed onto the forearm, their coordinates $\boldsymbol{A}_1^{(S1)}$ and $\boldsymbol{\omega}_{FE}^{(S1)}$ with respect to the frame S1 (sensor 1 is also fixed on the forearm) are *constant*. Similarly, also $\boldsymbol{A}_2^{(S2)}$ and $\boldsymbol{\omega}_{RUD}^{(S2)}$ are unknown but constant vectors.

For numerical calculations, we shall like to express (9) with respect to the base frame (B). Orientation matrices R_1 and R_2 from, respectively, sensors S1 and S2 can be used to transform coordinates from (S1) or (S2) to (B), e.g. for a general vector:

$$\boldsymbol{X}^{(B)} = R_1 \boldsymbol{X}^{(S1)} = R_2 \boldsymbol{X}^{(S2)} \tag{10}$$

Furthermore, due to inherent measurement noise, equation (9) will not hold exactly but in general we can write

$$\epsilon \;=\; \left| \boldsymbol{P}_2^{(B)} - \boldsymbol{P}_1^{(B)} - \boldsymbol{A}_1^{(B)} - \boldsymbol{\Delta}^{(B)} + \boldsymbol{A}_2^{(B)} \right|$$

and after a change of coordinates as in (10):

$$\begin{aligned} \epsilon \;=\; & \Bigg| \boldsymbol{P}_2^{(B)} - \boldsymbol{P}_1^{(B)} - R_1 \boldsymbol{A}_1^{(S1)} \dots \\ & \dots - \Delta \frac{R_1 \boldsymbol{\omega}_{FE}^{(S1)} \times R_2 \boldsymbol{\omega}_{RUD}^{(S2)}}{\left| R_1 \boldsymbol{\omega}_{FE}^{(S1)} \times R_2 \boldsymbol{\omega}_{RUD}^{(S2)} \right|} + R_2 \boldsymbol{A}_2^{(S2)} \Bigg| \end{aligned} \tag{11}$$

where ϵ is a positive scalar (ideally $\epsilon \to 0$).

It should be noticed that all terms in equation (11) are either directly measured from sensors ($\boldsymbol{P}_1^{(B)}$, $\boldsymbol{P}_2^{(B)}$, R_1, and R_2) or as unknown constants: one scalar Δ, two position vectors $\boldsymbol{A}_1^{(S1)}$, $\boldsymbol{A}_2^{(S2)}$, and two axes $\boldsymbol{\omega}_{FE}^{(S1)}$, $\boldsymbol{\omega}_{RUD}^{(S2)}$). Each position vector amounts to 3 unknown scalar parameters, defined as (7).
Each axis vector is by definition of unit length and amounts to only two unknown parameters. Guided by the clinical application, we decided to consider the sensors S1 and S2 as mounted on the dorsal part of the forearm and hand, respectively, with the wires directed proximally (see Fig. 1). For the specific case of Polhemus sensors, the sensor x-axis (aligned with the wire) will be roughly aligned with the main axes of the forearm (for S1) and hand (for S2). The z-axis of each sensor will point volarly (Fig. 1.a) . With this convention, we can define vectors of unit length identify with only two parameters[3], as follows:

$$\boldsymbol{\omega}_{FE}^{(S1)} \;:=\; \frac{1}{\sqrt{1+\alpha_1^2+\beta_1^2}} [\alpha_1 \ 1 \ \beta_1]^T \tag{12}$$

$$\boldsymbol{\omega}_{RUD}^{(S2)} \;:=\; \frac{1}{\sqrt{1+\alpha_2^2+\beta_2^2}} [\alpha_2 \ \beta_2 \ 1]^T \tag{13}$$

Similarly to [10], for a given set of measurements acquired during a time $t \in [0 \ T]$, we can determine the 11 parameters by solving a least-squares problem[4]

$$p^* := \underset{p \in \mathbb{R}^{11}}{\operatorname{argmin}} \frac{1}{T} \int_0^T \epsilon^2 \, dt$$

where $p := [A_{1x} \ A_{1y} \ A_{1z} \ A_{2x} \ A_{2y} \ A_{2z} \ \alpha_1 \ \beta_1 \ \alpha_2 \ \beta_2 \ \Delta]^T$ and ϵ is from (11).

B. Synthetic Data

Given a sequence of joint angles $\theta_{FE}^{(n)}$ and $\theta_{RUD}^{(n)}$, where n is the (discrete) time index, we can generate the corresponding sequence of wrist motions via the forward kinematic model. In particular, from eq. (2–4), we can generate the sequence of matrices ${}^{B}T_{S2}^{(n)}$ representing the sensor readings from S2. For the sensor S1, we assume that the forearm is at rest, therefore the sensor readings from S1 would be constant.

A pure FE movement is generated by keeping $\theta_{RUD}^{(n)} = 0$ while varying the FE joint angle $\theta_{FE}^{(n)}$. In particular, for a given number of samples N_s, $\theta_{FE}^{(n)}$ assumes N_s equally spaced values within its range of motion and $n = 1, \dots, N_s$. Similarly, for pure RUD movements, the FE joint angle is kept fixed while the RUD joint angle is varied between N_s equally spaced values within the RUD range of motion.

We simulated the effect of joint covariations by admitting motion for the joint supposedly held fixed. For example, for pure FE movements, we allowed $\theta_{RUD}^{(n)} = c\,\mu^{(n)}\,\theta_{FE}^{(n)}$, where c is a coefficient of covariation ($c = 0$ denotes a pure FE movement) and $\mu^{(n)}$ is a sequence of random numbers equally distributed between zero and one. A similar procedure was adopted for the RUD movements.

We then used both methods M1 and M2 to estimate the model parameters (A_1, A_2 and Δ) from sequences of FE

[3]The problem is similar to the parameterization of a 2-sphere which, although bidimensional, cannot be described (globally) with only two parameters. Equations (12) or (13) can only describe (almost) an hemisphere which becomes sufficient when the axis of a sensor is 'roughly' aligned with the expected direction of the anatomical axis.

[4]Numerically solved via the function `lsqnonlin` in MATLAB.

and RUD movements affected by different levels of joint covariations as well as by different number of samples N_s.

Finally, to simulate the effect of noisy measurements, we added noise ($\delta R^{(n)}$) to the orientation readings from the sensors, $R^{(n)}$, by $R^{(n)}_{noise} := \delta R^{(n)} R^{(n)}$. We considered three levels of angular RMS noise: $0.15°$, $0.30°$ and $0.45°$. The $0.15°$ level corresponds to the static accuracy orientation for the Polhemus Liberty System.

To assess accuracy and repeatability for each method in estimating a generic parameter A, we computed the relative error e_A, defined as

$$e_A = \frac{||\boldsymbol{A}_{est} - \boldsymbol{A}_{real}||}{||\boldsymbol{A}_{real}||} \tag{14}$$

where $\boldsymbol{A}_{est}$ and $\boldsymbol{A}_{real}$ are, respectively, the estimated and exact value of the parameter A.

C. Experimental data

We used the mock-up shown in Fig. 1.b, to conduct two batches of experiments. For each experiment, one subject was asked to manually move the mock-up (as if it were a patient's wrist, according to specific instructions described next) while the corresponding sequences of sensor readings ${}^{B}T_{S1}$, ${}^{B}T_{S2}$ were sampled at 240 Hz. Assuming the configuration of mock-up shown in Fig. 1.b as natural position, the movements started from this position.

1) Experiment 1 (Strapped forearm condition): The mock-up was mounted on a table, simulating a strapped forearm (in this case sensor S1 is not moving, providing constant readings). Three types of movements were performed:

Exp1a: one joint at a time was mechanically locked (with ad-hoc screws) while the subject was asked to perform 10 rotations with the other joint, throughout the range of motion.

Exp1b: subject was asked to perform a similar set of movements as in Exp1a on one joint at a time while the other joint was mechanically unlocked. Despite the specific instruction of performing single-joint movements, subject would unavoidably elicit movements in both joints at the same time.

Exp1c: the subject was asked to induce circumduction movements of the wrist (clearly, the mock-up joints were both unlocked).

2) Experiment 2 (ambulatory condition): The subject was instructed to perform movements as in Exp1b and Exp1c while holding the whole (lightweight) mock-up in his own hands. In particular, the mock-up forearm was no longer strapped onto the table, corresponding to an ambulatory condition (readings from sensor S1 were no longer constant).

For each motion, we recorded the sequence of sensor readings and used methods M1 and M2 to estimate the desired parameters of mock-up (i.e. A_1, A_2 and Δ). We computed the relative error for estimated values in a samilar procedure as described in eq. 14.

IV. Results

A. Synthetic Data

Using the described synthetic data we could evaluate the effect of joint covariation, noise and number of samples on the accuracy of parameter estimation by methods M1 and M2. Fig. 2.a shows the effect of joint covariation on parameter estimation on both methods, for different levels of noise when a large number of samples was acquired (Ns=2500). Because of the large number of samples, both methods are rather insensitive to noise levels but method M1 is highly sensitive to the covariation index. In particular, method M1 displays a parabolic increase of accuracy error for small covariations (0-20%) and linear afterwards, while method M2 is accurate (almost zero accuracy error) throughout the whole range of covariations (0-40%).

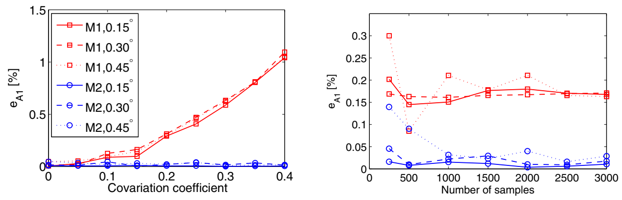

a) b)

Fig. 2. The effect of joint covariation(a) and the number of samples(b) on relative error in estimations of methods M1 (squares) and M2 (circles). The solid line, dashes and dots present $0.15°$, $0.30°$ & $0.45°$ angular RMS noise.

On the other hand, as shown in Fig. 2.b, both methods M1 and M2 are sensitive to noise for smaller numbers of samples (Ns $\leq$ 2000), only for larger samples (Ns $\geq$ 2500) the effect of noise on measurements is averaged out.

B. Experimental data

Experimental data with a mock-up were meant to highlight the joint covariation necessarily induced by manual movements on joints kinematically similar to the human wrist. Fig. 3 shows the joint-space representation of induced wrist movements. It is clear that in absence of locking mechanisms (screws for our mock-up, or possibly ad-hoc splinting for the human wrist) a joint covariation as large as 10% can be induced by manual motion of the wrist. Fig. 3 shows the superposition of 3 movements out of the 10 (for sake of clarity in the graph) in three different conditions. In the locked condition (solid line) the movements are perfectly superimposed, for the single-joint but unlocked condition (dotted lines) a 10% joint covariation is observed, a similar variability is present in the circumduction movements (dashed lines).

Another feature is that the centres of the 'crosses' relative the unlocked movements also display a 10% variability, indicating that with manual movements we should expect a repeatability error also for returning to a 'zero-position'.

The mean and standard deviation of the relative error for each trial is calculated to evaluate the accuracy (mean) and repeatability (standard deviation) of the methods M1 and M2 in parameter estimation. For method M2, the relative error on estimation is less than 7% for the parameters in all movements, showing a better accuracy than method M1, see Fig. 4). The accuracy in estimating Δ by method M2 seems insensitive to type of movement for both *strapped forearm* and

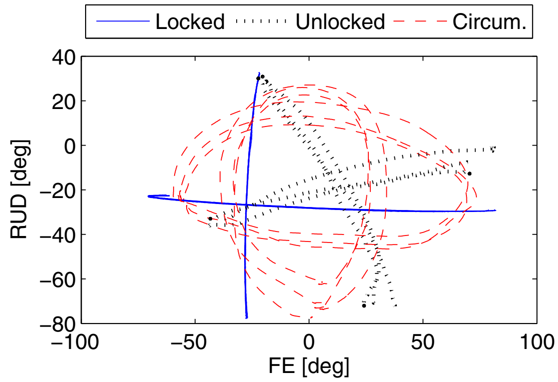

Fig. 3. Considering different joint rotations for 'Locked', 'Unlocked' and 'Circumduction' movements.

ambulatory conditions while, method M1 is highly related to the type of movement (Fig. 4). As it is expected, accuracy and repeatability in parameter estimation by method M1 in the locked conditions (i.e. mechanically induced pure single-joint movements) are better than or comparable with method M2.

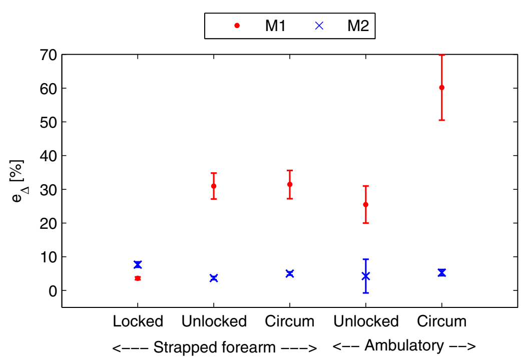

Fig. 4. Mean and standard deviation of relative error for estimating Δ, as a representative parameter of the physical mock-up, by methods M1 (dots) and M2 (crosses).

V. Conclusion

In this paper we first evaluated the effect of joint covariation, number of samples as well as noise in measurements on the outcome of two types of parameter estimation methods: method M1 proposed by Biryukova et al. [10] and method M2 adapted from Prokopenko et al. [12]. To this end, we used synthetic data to artificially change the amount of joint covariation and level of noise, in relation of number of samples. For method M1, which assumes pure single-joint motions, the accuracy error increases with joint covariation while method M2 is insensitive to joint covariation, see Fig. 2.a. However, both methods are sensitive to noise in measurements, especially for lower number of samples (less than 2500 per movement), as shown in Fig. 2.b.

To assess the accuracy and repeatability of methods M1 and M2, we developed a physical mock-up with known dimensions to be able to compare the estimated values with the actual ones (i.e. estimating accuracy). We computed the mean (accuracy) and standard deviation (repeatability) of relative errors for the parameter estimation for both *strapped forearm* and *ambulatory* conditions. As expected, in general, method M2 outperforms method M1 in terms of repeatability and accuracy except for the locked condition, in which joint covariation is inhibited, see Fig. 4.

This preliminary study shows that method M2 is especially suitable for ambulatory conditions where higher variability in the joint space (e.g. joint covariation or circumduction movements) induces better accuracy in parameter estimation. As for future work, we aim at deriving guidelines for a clinical protocol, to guarantee a given level of accuracy in estimating the parameters of human wrist joints.

References

[1] G. Welch and E. Foxlin, "Motion tracking: no silver bullet, but a respectable arsenal," *Computer Graphics and Applications, IEEE*, vol. 22, no. 6, pp. 24–38, 2002.

[2] A. Cutti, A. Giovanardi, L. Rocchi, A. Davalli, and R. Sacchetti, "Ambulatory measurement of shoulder and elbow kinematics through inertial and magnetic sensors," *Medical and Biological Engineering and Computing*, vol. 46, no. 2, pp. 169–178, 2008.

[3] L. Leonard, D. Sirkett, G. Mullineux, G. Giddins, and A. Miles, "Development of an in-vivo method of wrist joint motion analysis," *Clinical Biomechanics*, vol. 20, no. 2, pp. 166–171, 2005.

[4] D. Campolo, D. Formica, E. Guglielmelli, and F. Keller, "Kinematic analysis of the human wrist during pointing tasks," *Experimental brain research*, vol. 201, no. 3, pp. 561–573, 2010.

[5] N. Tagliamonte, M. Scorcia, D. Formica, F. Taffoni, D. Campolo, and E. Guglielmelli, "Force control of a robot for wrist rehabilitation: Coping with human motor strategies during pointing tasks," *RSJ Advanced Robotics Journal*, vol. 25, pp. 537–562, 2011.

[6] D. Campolo, D. Accoto, D. Formica, and E. Guglielmelli, "Intrinsic constraints of neural origin: Assessment and application to rehabilitation robotics," *Robotics, IEEE Trans on*, vol. 25, no. 3, pp. 492–501, 2009.

[7] F. Sergi, D. Accoto, D. Campolo, and E. Guglielmelli, "Forearm orientation guidance with a vibrotactile feedback bracelet: On the directionality of tactile motor communication," in *Biomedical Robotics and Biomechatronics, 2008. 2nd IEEE RAS & EMBS International Conference on*, pp. 433–438.

[8] D. Campolo, F. Widjaja, M. Esmaeili, and E. Burdet, "Pointing with the wrist: a postural model for donders' law," *Experimental Brain Research*, DOI: 10.1007/s00221-011-2747-3, 2011.

[9] J. Andrews and Y. Youm, "A biomechanical investigation of wrist kinematics," *Journal of Biomechanics*, vol. 12, no. 1, pp. 83–93, 1979.

[10] E. V. Biryukova, A. Roby-Brami, A. A. Frolov, and M. Mokhtari, "Kinematics of human arm reconstructed from spatial tracking system recordings," *Journal of Biomechanics*, vol. 33, no. 8, pp. 985–995, 2000.

[11] J. OBrien, R. Bodenheimer Jr, G. Brostow, and J. Hodgins, "Automatic joint parameter estimation from magnetic motion capture data," *Proceedings of Graphics Interface*, pp. 53–60, 2000.

[12] R. A. Prokopenko, A. A. Frolov, E. V. Biryukova, and A. Roby-Brami, "Assessment of the accuracy of a human arm model with seven degrees of freedom," *Journal of Biomechanics*, vol. 34, no. 2, pp. 177–185, 2001.

[13] N. Rezzoug, J. Jacquier-Bret, and P. Gorce, "A method for estimating three-dimensional human arm movement with two electromagnetic sensors," *Computer Methods in Biomechanics and Biomedical Engineering*, vol. 13, no. 6, pp. 663–668, 2010.

[14] Z. Li, L. Kuxhaus, J. A. Fisk, and T. H. Christophel, "Coupling between wrist flexion-extension and radial-ulnar deviation," *Clinical Biomechanics (Bristol, Avon)*, vol. 20, no. 2, pp. 177–183, 2005.

[15] R. Murray, Z. Li, , and S. Sastry, *A mathematical introduction to robotic manipulation*. CRC, 1994.